

The influence of discharge power and heat treatment on calcium phosphate coatings prepared by RF magnetron sputtering deposition

Yan Yonggang · J. G. C. Wolke · Li Yubao · J. A. Jansen

Received: 2 September 2005 / Accepted: 8 March 2006 / Published online: 1 February 2007
© Springer Science+Business Media, LLC 2007

Abstract Ca–P coatings with different Ca/P ratio and composition were successfully prepared by RF magnetron sputtering deposition. The Ca/P ratio, phase composition, structure and morphological properties were characterized by XRD, FTIR, EDS and SEM analyses. All the as-sputtered coatings were amorphous and after IR-irradiation the coatings altered into a crystalline phase. The obtained coatings had a Ca/P ratio that varied from 0.55 to 2.10 and different phase compositions or mixtures of apatite, beta-pyrophosphate and beta-tricalciumphosphate structures were formed. Evidently, the phase compositions of the sputtered coatings are determined not only by the discharge power ratio of the hydroxylapatite and calcium pyrophosphate targets but also by the annealing temperature.

Introduction

In the biomedical field, coatings are frequently applied onto the surface of metallic dental and orthopaedic

implants in order to improve their biological performance. Because of its similarity to the inorganic component of bone and teeth, calcium phosphate (CaP) ceramics are considered as a suitable class of materials for use as a surface coating [1]. Therefore, CaP coatings on metallic substrates have been developed, which are currently used in loaded situations, like total joint replacements and dental root implants. In this way the mechanical strength of titanium and the biocompatibility of CaP are combined [2].

As demonstrated in various publications, CaP coatings show a favourable bone response compared with non-coated titanium implants. At the moment, various techniques are available for the deposition of calcium phosphate on metal implants [3–11]. Over the past few years, we have made use of an RF magnetron sputter coating technique to produce thin adherent CaP coatings on implants. The results showed that the deposited films had a good biological response, both in vitro and in vivo. The osteogenic capacity of CaP was shown to be dependent on the physicochemical properties, such as the coating composition, coating crystal as well as molecular structure and coating crystallinity [12–19]. However, the final bone response can also be influenced by the structural arrangement of calcium phosphate ceramics, and besides HA other calcium phosphate ceramics like calcium phosphate and calcium pyrophosphate play a role in the mechanism for the formation of a carbonated-apatite deposit. The capacity of biomaterials to initiate the formation of a carbonated-apatite layer is indicative for their bioactivity [20–23].

In view of the above-mentioned, previous studies in our laboratory demonstrated that the dissolution behaviour in simulated body fluid (SBF) of RF

Y. Yonggang · J. G. C. Wolke (✉) · J. A. Jansen
Department of Periodontology and Biomaterials, Radboud University Nijmegen Medical Center, PO Box 9101, 6500 HB Nijmegen, The Netherlands
e-mail: J.Jansen@dent.umcn.nl

Y. Yonggang · L. Yubao
Department of Nano-biomaterials Center, Analytical and Testing Center, Sichuan University, Chengdu 610064, P. R. China

magnetron sputtered calcium pyrophosphate (DCPP) coatings was similar as compared to HA coatings. Further, rat bone marrow stromal cells proliferated and differentiated only on crystalline magnetron sputtered DCPP as well as HA coatings, while crystalline HA coatings induced an earlier osteogenic effect than the crystalline DCPP coatings [24]. Despite these favourable results, it has to be noticed that the physicochemical evaluation of pyrophosphate coatings is not as well studied as those of calcium phosphate coatings. Especially, investigations of mixtures of both materials are scarce.

Therefore, the objective of the present study was to characterize the physicochemical properties of calcium pyrophosphate and hydroxylapatite coatings obtained by RF magnetron sputtering.

Materials and methods

Ca–P coating deposition

For the experiments commercially pure titanium (cpTi) discs were provided with various Ca–P sputter coatings. The discs measured 1 mm in thickness and had a diameter of 12 mm. All discs were Al₂O₃-blasted on one side.

RF magnetron sputter coatings were made by using a commercially available RF sputter deposition system provided with two separate targets (Edwards ESM 100). The target materials were calcium pyrophosphate (β -Ca₂P₂O₇) and hydroxylapatite (Ca₅(PO₄)₅OH) granules (diameter 0.5–1.0 mm). The test specimens were mounted on a rotating and water-cooled substrate holder. The distance between target and substrate was 80 mm and the target–target distance was 25 mm. Before sputtering the metal substrates were cleaned by etching for 10 min with argon ions. During deposition, the argon pressure was kept at 5×10^{-3} mbar and the deposition time was 430 min. The composition of the target materials were characterized after sputtering by energy dispersive spectroscopy (Table 1).

In total five coating groups were prepared:

- (1) HA; at a discharge power of 400 W for both targets.

- (2) Mixture HA/Pyro; at a discharge power of 600 W for the HA target and 200 W for DCPP target.
- (3) Mixture HA/Pyro; at a discharge power of resp. 400 W and 400 W.
- (4) Mixture HA/Pyro; at a discharge power of resp. 200 W and 600 W.
- (5) Pyro; at a discharge power of 400 W for both targets.

Coating thicknesses of 2 μ m were produced and the deposition rate for Pyro and HA were analyzed with a step measurement. The coating was deposited on a silicon wafer (10 \times 10 \times 0.5 mm), half of the wafer was covered with a tape. After the coating procedure the tape was removed and the thickness of the coating was measured using a Universal Surface Tester (UST, Innowep GmbH, Germany). Briefly, the instruments worked as follows. A diamond stylus scanned mechanically the surface along a straight line and the vertical deflection of the stylus was registered. The results are listed in Table 2.

After deposition, half of the coated specimens were subjected to an additional infrared heat treatment (HT) for 30 s at 550, 650 and 750 °C (Quad Ellipse Chamber, Model E4-10-P, Research Inc.).

Characterization of sputtered coatings

Before and after annealing, coatings were characterized as follows:

- The crystallographic structure of each film was determined by thin film X-ray diffraction (XRD) using a Philips θ – 2θ diffractometer (PW 3710, 40 kV, 40 mA) using a CuK α -radiation of 1.5418 Å wavelength. For these measurements the specimens were scanned from 20–39° 2θ at a scanning speed of 0.008°/s and a stepsize of 0.01° 2θ .
- The infrared spectra of the films on the substrates were obtained by reflection Fourier transform infrared spectroscopy (FTIR) (Spectrum One, Perkin-Elmer), since infrared radiation cannot pass through the titanium substrate. The coatings were analyzed in the range 4000–400 cm^{–1} at 2 cm^{–1} resolution and 16 scans. All spectra were recorded at ambient temperature.

Table 1 Ca/P ratio of the target material after sputtering of the Ca–P coatings

	Ca/P ratio surface	Ca/P ratio starting material
HA	1.1	1.67
Pyro	1.56	1.0

Table 2 Deposition rate of the films deposited at different discharge power level on a rotated substrate holder

	200 W	400 W	600 W
HA (nm/h)	70	141	210
Pyro (nm/h)	68	140	208

- The surface topology of the films was examined using scanning electron microscopy (SEM) using a Jeol 6310 SEM at an accelerating voltage of 10 kV after Au coating.
- The above-described scanning electron microscope was equipped with an energy-dispersive X-ray microanalyzer (voyager) EDS was carried out at a magnification of 500× at an accelerating voltage of 10 kV in order to determine the elemental composition of deposited coatings. Stoichiometric hydroxylapatite discs of known Ca/P ratio and of equal thickness to the coated Ti-substrates (1.5 mm) were used as a reference for the determination of Ca/P ratios of the deposited Ca/P coatings.

Theoretical Ca/P ratio was calculated as follow:

$$R_{\text{Ca/P}} = R_{\text{HA}} \frac{P_{\text{HA}}}{P_{\text{HA}} + P_{\text{Pyro}}} + R_{\text{Pyro}} \frac{P_{\text{Pyro}}}{P_{\text{HA}} + P_{\text{Pyro}}}$$

$R_{\text{HA}} = 1.67$, $\text{Ca}_{10}(\text{PO}_4)_6(\text{OH})_2$; $R_{\text{Pyro}} = 1.0$, $\text{Ca}_2\text{P}_2\text{O}_7$; P_{HA} : discharge power HA; P_{Pyro} : discharge power pyrophosphate.

Results

X-ray diffraction

The XRD patterns of the as-sputtered coatings showed an amorphous structure with no clear peaks, besides the underlying substrate peaks also a peak of the Al_2O_3 blasting material at 25.6° (2-Theta) was visible (Fig. 1a–d).

At 550°C , the amorphous coating HA was transformed into a crystalline apatite structure with main reflection lines at (002), (211) and (112), which correspond to peaks at 25.9° , 31.9° and 32.4° (2-Theta). The amorphous HA/Pyro (600 W/200 W) changed into two crystalline phases, an apatite structure with peaks at 25.9° , 31.9° and 32.4° (2-Theta) and a beta-calcium pyrophosphate structure with peaks at 26.6° , 27.7° and 29.5° (2-Theta). HA/Pyro (400 W/400 W) coatings alter into three crystalline phases, an apatite structure with peaks at 25.9° , 31.9° and 32.4° (2-Theta), a beta-calcium pyrophosphate structure with peaks at 26.6° , 27.7° and 29.5° (2-Theta) and a beta-tricalcium phosphate structure with peaks at 25.9° , 27.7° and 31° (2-Theta). For the amorphous HA/Pyro (200 W/600 W) the formation of beta-calcium pyrophosphate could be detected, with peaks at 26.6° , 27.7° and 29.5° (2-Theta).

On the other hand, the Pyro coating remained unchanged and required a higher infrared heat-treatment to obtain crystallization (Fig. 1a–d).

After heat treatment at 650°C , the heated HA, HA/Pyro (600 W/200 W), HA/Pyro (400 W/400 W) and HA/Pyro (200 W/600 W) coatings showed the same results as the coatings heated at 550°C , while the amorphous Pyro coatings changed into a crystalline beta-calcium pyrophosphate structure with reflections lines 201, 202, 008 and 212, which correspond to peaks at 26.6° , 27.7° , 29.5° and 30.7° (2-Theta). For all the coatings heated at 750°C the formation of TiO_2 with peaks at 27.6° and 36.0° (2-Theta) appeared, and also peaks developed around 27.7° and 31° during the heat treatment, which attributed to beta-TCP formation

The X-ray diffraction data of all the heat-treated coatings are listed in Table 3.

FTIR spectroscopy

As-sputtered coatings

Fourier transform infrared spectroscopy measurements showed for all the amorphous coatings two clusters of bands from 900 to 1200 and from 500 to 600 cm^{-1} attributed to the major absorption modes associated with the presence of phosphate (Fig. 2a–d).

Infrared heat-treatment at 550°C

Fourier transform infrared spectroscopy of the HA coatings resulted in the appearance of the hydroxyl band at 630 cm^{-1} , characteristic for hydroxylapatite and the appearance of various P–O bonds at a wavelength of 567, 587, 965, 1009, 1083 cm^{-1} and two small absorptions at 1408 and 1464 cm^{-1} were related to carbonate ions substituting for phosphate groups (B-type). The FTIR of the heat treated HA/Pyro (600 W/200 W) and HA/Pyro (400 W/400 W) coatings showed identical FTIR as the HA coatings, with the absence of carbonate peaks. The HA/Pyro (200 W/600 W) coatings revealed characteristics of a mixture of apatite and beta-calcium pyrophosphate phases with various P_2O_7 bonds at 555, 606, 921, 951, 999, 1023, 1053, 1096, 1131, 1148, 1166 and 1204 cm^{-1} and PO_4 bonds at 562, 962, 1035 and 1065 cm^{-1} . The Pyro coatings resulted in the appearance of various P_2O_7 bonds at the wavelength around 550, 595, 950, 998, 1025, 1055, 1088, 1125, 1163 and 1202 cm^{-1} , which are characteristic for the beta-calcium pyrophosphate structure [21].

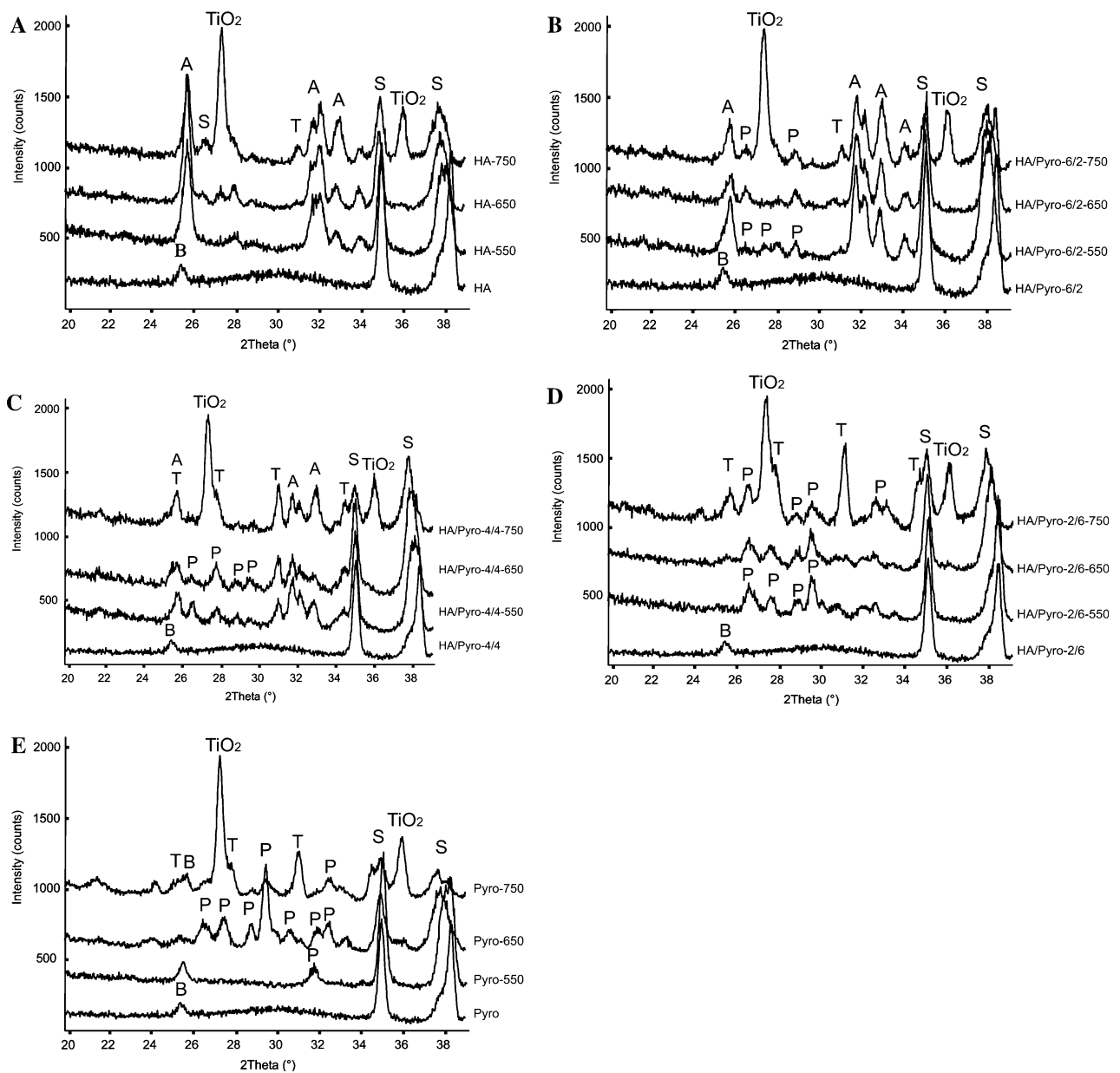
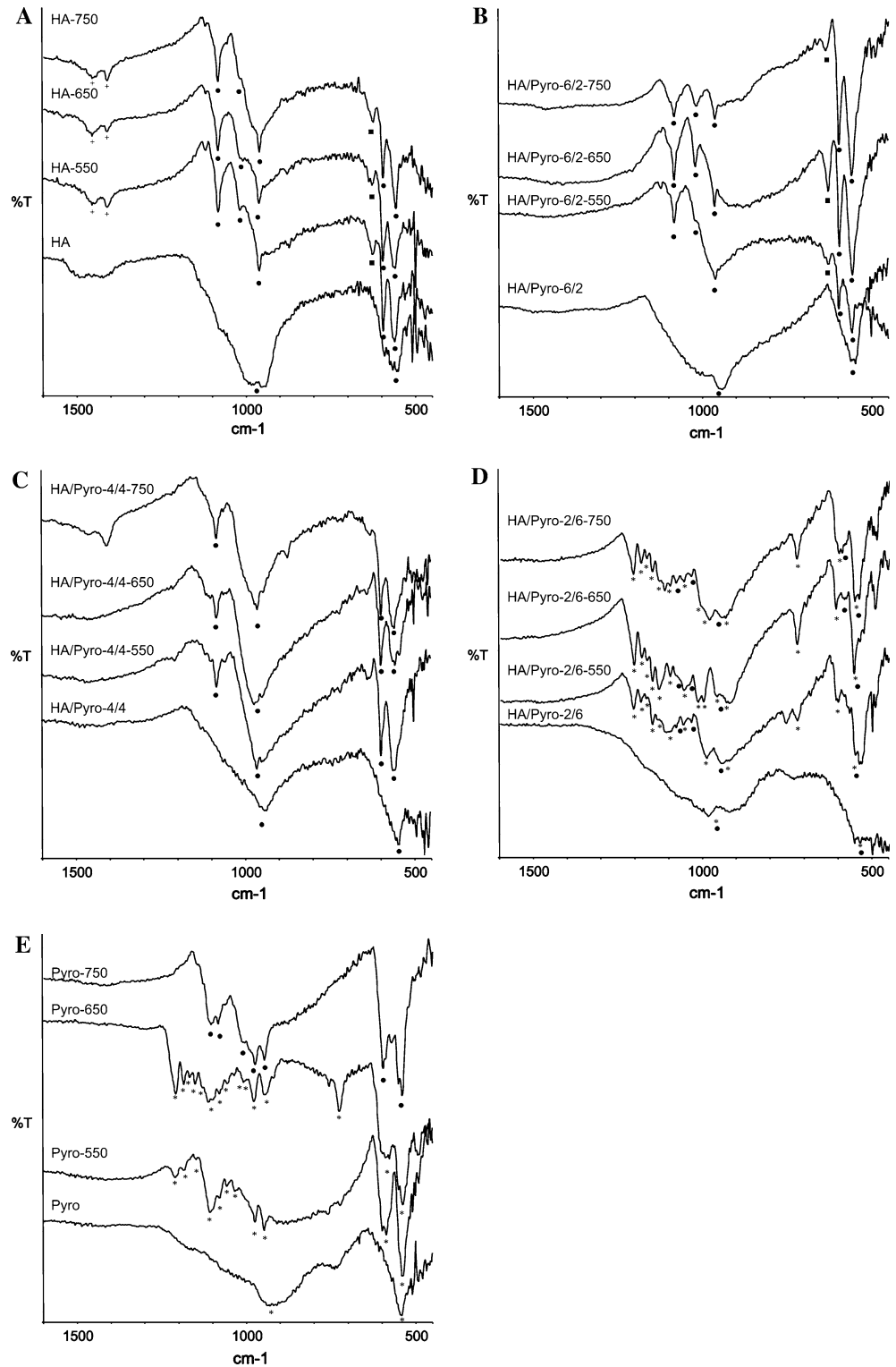


Fig. 1 (a–d) XRD patterns of as-sputtered and heat treated coatings (A: apatite, P: calcium pyrophosphate, T: beta-tricalcium phosphate, TiO₂: titaniumoxide, S: titanium substrate and B: Al₂O₃ blasting material)

Table 3 The phase composition of the sputtered coatings at different discharge power ratio at different annealing temperature from XRD analysis

Discharge power (HA:Pyro: w/w)	550 °C	650 °C	750 °C
2× 400:0	HA	HA	HA + TCP + TiO ₂
600:200	HA + Pyro	HA + Pyro	HA + Pyro + TCP + TiO ₂
400:400	HA + Pyro + TCP	HA + Pyro + TCP	HA + TCP + TiO ₂
200:600	Pyro	Pyro	Pyro + TCP + TiO ₂
0:2× 400	–	Pyro	Pyro + TCP + TiO ₂

Fig. 2 (a–d) FTIR spectra of as-sputtered and heat treated coatings. ((●) PO₄, (*) P₂O₇, (■) OH and (+) CO₃)



Infrared heat-treatment at 650 °C

Fourier transform infrared spectroscopy showed identical FTIR spectra as obtained after the heat treatment at 550 °C.

Infrared heat-treatment at 750 °C

At this temperature only a change of the Pyro coating could be observed. The spectrum showed various P–O bonds at the wavelength around 551, 596, 947, 975,

1011, 1079 and 1115 cm^{-1} , which are characteristic for the beta-tricalcium phosphate.

Scanning electron microscopy

Scanning electron microscopy examination showed that, besides the HA/Pyro (200 W/600 W) coating, all the other amorphous coatings resulted in a uniform coverage of the titanium substrate. In contrast, the HA/Pyro (200 W/600 W) had a different morphology, i.e., the surface crystals grew vertically on top of the coating (Fig. 3g).

Scanning electron microscopy revealed that at 550 °C no changes of the morphology of heated coatings were observed. On the other hand, at 650 °C the HA/Pyro (200 W/600 W) and the Pyro coatings changed in morphology (Fig. 3a–f). During the heat treatment the plate-like crystals of the HA/Pyro (200 W/600 W) disappeared (Fig. 3h). The surface

morphology of the heated Pyro coating was characterized by a flat appearance with micropores and needle-like crystals (Fig. 3j). At 750 °C, no further change in the morphology could be found.

EDS analysis of the different coatings are listed in Table 4.

Discussion

The aim of this study was to investigate the applicability of RF magnetron sputtering for the production of mixtures of hydroxylapatite and calcium pyrophosphate coatings on titanium substrates. The results demonstrated that it is possible to deposit dense and adherent mixtures of hydroxylapatite and calcium pyrophosphate coatings by choosing the appropriate deposition parameters.

Fig. 3 (a–j) SEM micrographs of Ca–P coatings, as-sputtered and heat treated at 650 °C. (1000×)

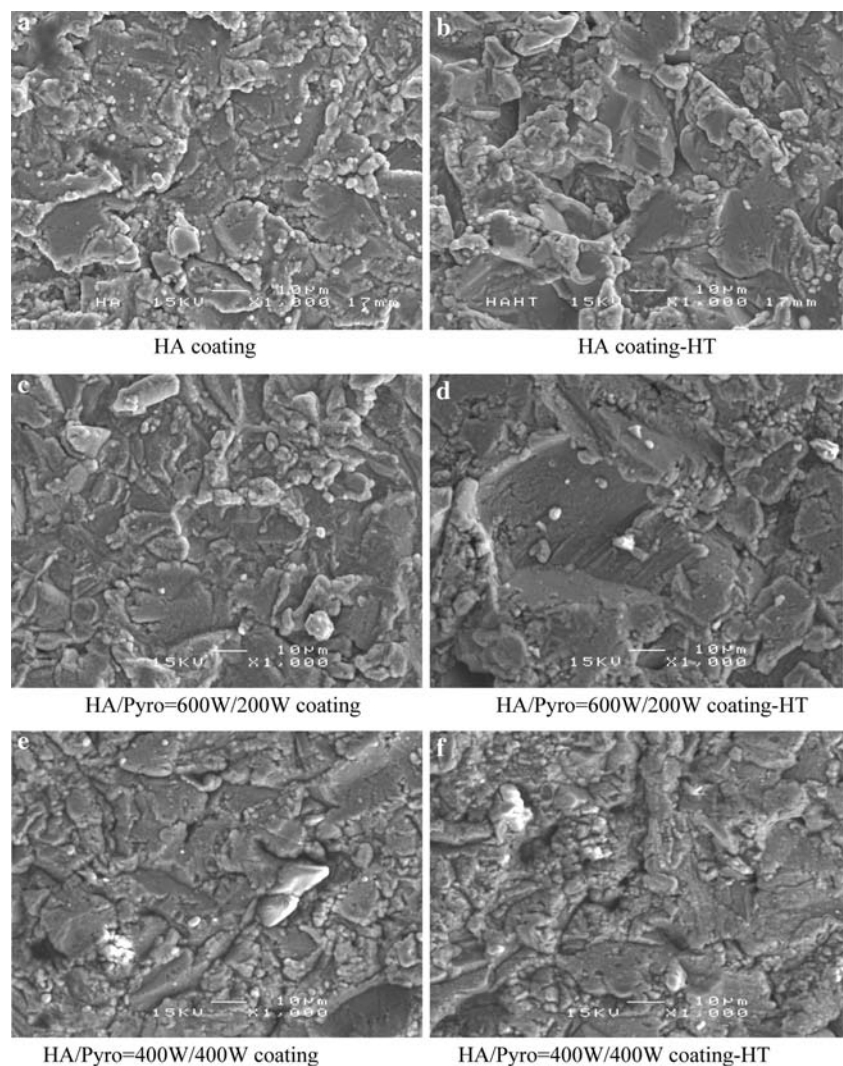
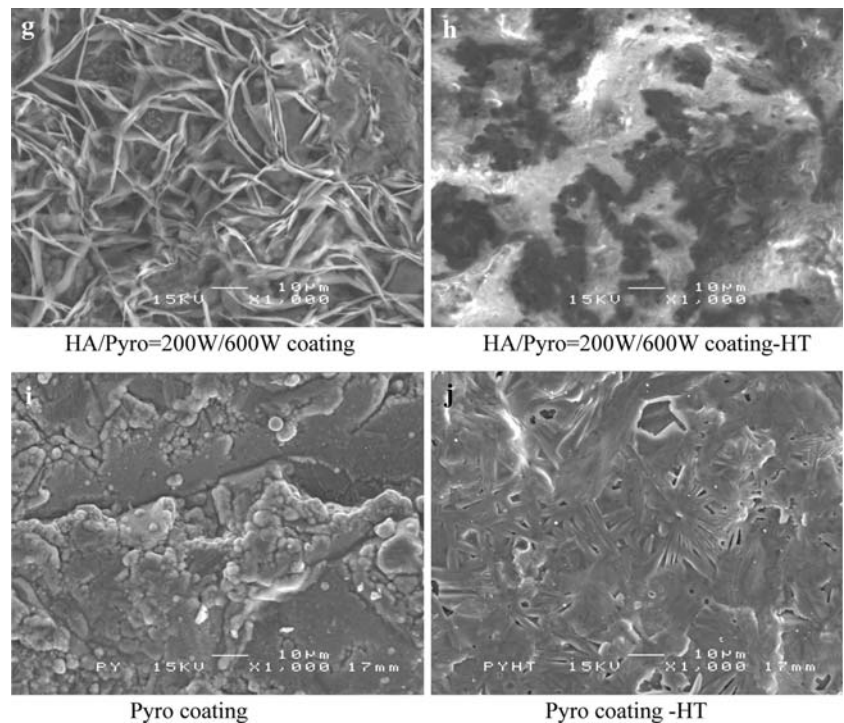


Fig. 3 continued



RF magnetron sputter deposition is a rather complex process to describe in physical parameters, especially when used to sputter multi-compounds like hydroxylapatite and pyrophosphate. There are, besides target composition, two main process parameters, which can be varied to influence the physical and chemical properties of the coating: working gas pressure and discharge power. In our study, we changed the discharge power and the Argon pressure was kept constant. In literature, there is discrepancy about the exact process of building a layer. It is generally accepted that during the sputtering process the deposited layers are build up atom for atom or ion for ion. Although other researchers found that particles are ejected as a neutral and as a negatively particle, they suggested that phosphorus and calcium were ejected as neutral, while oxygen was escaped from the target as a negative ion [25]. We observed

that besides all the mentioned particles, also phosphate groups are sputtered. XRD revealed that a mixture of crystalline pyro and hydroxylapatite coatings (400 W/400 W) consisted of an apatite, beta-pyrophosphate and beta-tricalciumphosphate structure. The Ca/P ratio of this coating is 1.5, when a coating is build up from atoms or ions, the heat treatment of this coating will only result in the formation of a tricalcium phosphate. In this study, we found a mixture of several phases and therefore we assume that molecules and clusters of ortho- and pyrophosphate materials play an important role in building a calcium phosphate layer.

The EDS analysis showed that the Ca/P ratio of the sputtered coatings was higher than the theoretical values for HA and HA/Pyro (600 W/200 W and 400 W/400 W) coatings and lower for the HA/Pyro (200 W/600 W) and Pyro coatings. Concerning the high Ca/P ratio of the coatings, several studies have been

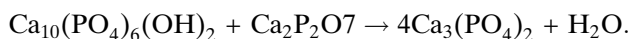
Table 4 Ca/P ratio of all the sputtered and heat treated coatings

Discharge power (HA:Pyro: w/w)	Ca/P amorphous coating	Ca/P heat treated 550 °C	Ca/P heat treated 650 °C	Ca/P heat treated 750 °C	Calculated Ca/P
2× 400:0	2.00	2.00	2.01	2.10	1.67
600:200	1.82	1.84	1.82	1.85	1.50
400:400	1.51	1.53	1.49	1.55	1.34
200:600	0.55	0.57	0.56	0.88	1.17
0.2× 400	0.76	0.78	0.78	1.19	1.00

published where preferential sputtering of calcium was observed, probably due to the possibility of the phosphorus ions being pumped away before they are deposited on the substrate [26]. An explanation for the decrease in Ca/P ratio of the other coatings is the structure of the pyrophosphate anion. It has been published that pyrophosphates have a great tendency to occur in polymorphic phases and to consist of two PO₄ tetrahedral bridged by a mutual oxygen atom [27]. Consequently, we hypothesize that the possibility of pyrophosphate ions being pumped away during sputtering is very low, due to the complex structure as compared to the orthophosphate anion. Further, it has to be noticed that PO₄ reaches the substrate surface easier and is much more volatile than Ca ions [28, 29]. Also the impact of a particle with the target material may lead to structural rearrangements such as the introduction of interstitials or vacancies. It may also introduce lattice defects such as stoichiometry modifications. In our sputtering system, we observed a preferential sputtering of the outer layer of the target material; the Ca/P ratio of the pyrophosphate target increased in time from 1.0 to 1.56, while for the hydroxylapatite target material a decrease was found (1.67–1.1). It is clear that a cascade of events occurs during sputtering of calcium phosphate materials. As a result, the exact mechanism of how the sputtered layer is build up, is not completely understood. Therefore, research efforts in this area should have more attention.

Furthermore, the crystallization of the amorphous as sputtered coatings is depending on the temperature during infrared heating. At 650 °C or higher the XRD all the amorphous coatings showed a crystalline structure. Further, the post heat treatment at 750 °C resulted in an increase of thickness of the TiO₂ layer. This increase is not considered to be a disadvantage for the long-term bone response. It has already reported that the growth of the titanium oxide layer can even enhance the bonding to bone [30].

Finally, XRD analysis demonstrated that the mixing of HA and Pyro resulted in the formation of beta-tricalcium phosphate phase. From literature, it is known that apatite and pyrophosphate forms tricalcium phosphate around 650 °C according to the following reaction [31]:



It has been described that tricalcium phosphate is generally considered as a more resorbable biomaterial than dense hydroxylapatite and is used to overcome the low biodegradation of hydroxylapatite.

Conclusion

Based on the results of this study, it can be concluded that magnetron sputtering can be successfully used to deposit calcium pyrophosphate and hydroxylapatite coatings on metal substrates. All the as-sputtered coatings were amorphous and after IR-irradiation the coatings altered into a crystalline phase. The obtained coatings had a Ca/P ratio varying from 0.55 to 2.0 and different phase compositions or mixtures of apatite, beta-pyrophosphate and beta-tricalciumphosphate structures were formed. The phase compositions of the sputtered coatings are determined not only by the discharge power ratio of the hydroxylapatite and calcium pyrophosphate target, but also by the annealing temperature. These results suggest that magnetron sputtering of mixtures of apatite and calcium pyrophosphate coating is a promising method for forming a ceramic coating. Of course, the final bone biocompatibility of these coatings has to be proven in follow-up cell culture and experimental animal studies.

References

1. K. DE GROOT, C. P. A. T. KLEIN, J. G. C. WOLKE and J. M. A. DE BLIECK-HOGERVORST, in Handbook of Bioactive Ceramics, Vol. 2, edited by T. Yamamuro, L. L. Hench and J. Wilson, (1990) 3
2. M. M. A. AMSELAAR, F. C. M. DRIESSENS, W. KALK, J. D. De WIJN and P. J. Van MULLEN, *J. Mater. Med.* **2** (1991) 63
3. K. DE GROOT, R. GEESINK, C. P. A. T. KLEIN and P. SERELIAN, *J. Biomed. Mater. Res.* **21** (1987) 1375
4. H. L. BARTHELL, T. A. ARCHULETA and R. KOS-SOWSKY, *Mater. Res. Soc. Symp. Proc.* **110** (1989) 709
5. H. OGUCHI, K. ISHIKAWA, S. OJIMA, Y. HIRAYAMA, K. SETO and G. EGUCHI, *Biomaterials* **13** (1992) 471
6. P. DUCHEYENE, S. RADIN, M. HEUGHEBAERT and J. C. HEUGHEBAERT, *Biomaterials* **11** (1990) 244
7. K. RAJIV, F. SINGH, F. QIAN, V. NAGABUSHNAM, R. DAMMODARAN and B. M. MOUDGIL, *Biomaterials* **7** (1994) 522
8. C. M. COTELL, D. B. CHRISEY, K. S. GRABOWSKI and J. A. SPRAGUE, *Appl. Biomater.* **8** (1992) 87
9. T. YOSHINARI, Y. OHTSUKA and T. DERAND, *Biomaterials* **7** (1994) 528
10. J. G. C. WOLKE, J. M. A. De BLIECK-HOGERVORST, W. J. A. DHERT, C. P. A. T. KLEIN and K. DE GROOT, *J. Therm. Spray Techn.* **1**(1992) 79
11. J. A. JANSEN, J. G. C. WOLKE, S. SWANN, J. P. C. M. VAN DER WAERDEN, K. DE GROOT, *Clin. Oral Impl. Res.* **4** (1993) 28
12. N. KIVRAK, A. CUNEY, *J. Am. Ceram. Soc.* **81** (1998) 2245
13. P. HARDOUIN, D. CHOPIN, B. DEVYVER, B. FLAUTRE, M. C. BLARY, P. GUIGUI and K. ANSELME, *J. Mater. Sci. Med.* **3** (1991) 212
14. T. KTSUGI, T. YAMAMURO, T. NAKAMURA and M. OKA, *Biomaterials* **16** (1995) 1101

15. R. HYUN-SEUNG, Y. HYUK-JOON, H. KUG SUN, C. BONG-SUN, L. CHOON-KI and C. SUNG-SOO, *Biomaterials* **23** (2002) 909
16. J. S. SUN, Y. C. HUANG, Y. H. TSUANG, L. T. CHEN and F. H. LIN, *J. Biomed. Mat. Res.* **2** (2002) 246
17. P. DUCHEYNE, S. RADIN and L. KING, *J. Biomed. Mat. Res.* **27** (1993) 25
18. S. RADIN and P. DUCHEYNE, *J. Biomed. Mat. Res.* **27** (1993) 35
19. E.G. NORDSTRÖM, L. NIEMI and J. MIETTINEN, *Biomed. Mat. Eng.* **2** (1992) 115
20. H. S. CHEUNG, M. T. STORY and D. J. MCCARTY, *Arthritis Rheum.* **27** (1984) 668
21. S. KAMAKURA, Y. SASANO, H. HOMMA, O. SUZUKI, H. OHKI, M. KAGAYAMA and K. MOTEGI, *J. Dent. Res.* **78** (1999) 1682
22. K. VAN DIJK, H. G. SCHAEKEN, J. G. C. WOLKE, C. H. M MAREE, F. H. P. M. HABRAKEN, J. VERHOEVEN and J. A. JANSEN, *J. Biomed. Mat. Res.* **29** (1995) 269
23. K. YAMASHITA, T. ARASHI, K. KITAGAKI, S. YAMASA and T. UMEGAKI, *J. Am. Ceram. Soc.* **77** (1994) 2401
24. Y. YAN, J. G. C. WOLKE, Y. LI and J. A. JANSEN, *J. Biomed. Mater. Res.* **76A** (2006) 744
25. B. FEDDES, A. M. VREDENBERG, J. G. C. WOLKE and J. A. JANSEN, *J. Appl. Phys.* **93** (2003) 662
26. P. C. ZALM, in *Handbook of Ion Beam Processing Technology*, edited by J. J. CUOMO, S. M. ROSSNAGEL and H. R. KAUFMAN, (1989) 78
27. A. D. F. TOY, in *Comprehensive Inorganic Chemistry*, edited by J. C. BAILER, H. J. EMELEUS, R. NYHOLM and A. F. TROTMAN-Dickenson, Vol 2 (1973) 509
28. B. O. FOWLER, E. C. MORENO and W. E. BROWN, *Arch. Oral Bio.* **11** (1966) 477
29. J. P. SCHMITZ, J. O. HOLLINGER and S. B. MILAM, *J. Oral Maxillofac. Surg.* **57** (1999) 1122
30. T. KITSUGI, T. NAKAMURA, M. OKA, W. YAN, T. GOTO, T. SHIBUYA, T. KOKUBO and S. MIYAJI, *J. Biomed. Mater. Res.* **32** (1996) 149
31. S. KAMAKURA, Y. SASANO, T. SHIMIZU, K. HATORI, O. SUZUKI, M. KAGAYAMA and K. MOTEGI *J. Biomed. Mater. Res.* **59** (2002) 29